Chemistry & Biology
Article

Fluorescent Probes of Tissue Transglutaminase Reveal Its Association with Arterial Stiffening

Nicolas Chabot,[1] Simon Moreau,[2] Amina Mulani,[1] Pierre Moreau,[2] and Jeffrey W. Keillor[1,*]
[1]Département de chimie, Université de Montréal, C.P. 6128, Succursale centre-ville, Montréal, QC H3C 3J7, Canada
[2]Faculté de pharmacie, Université de Montréal, C.P. 6128, Succursale centre-ville, Montréal, QC H3C 3J7, Canada
*Correspondence: keillorj@chimie.umontreal.ca
DOI 10.1016/j.chembiol.2010.06.019

SUMMARY

Tissue transglutaminase (TG2) catalyzes the crosslinking of proteins. TG2 has been implicated in fibrosis and vascular calcification, both of which lead to a common feature of aging known as arterial stiffness. In order to probe the role of TG2 in arterial rigidification, we have prepared a fluorescent irreversible inhibitor as a probe for TG2 activity (RhodB-PGG-K(Acr)-LPF-OH). This probe was synthesized on solid support, characterized kinetically (k_{inact} = 0.68 min^{-1}, K_I = 79 μM), and then used to stain the aorta from rats used as a model of isolated systolic hypertension (ISH). Interestingly, TG2 activity was thus shown to increase over 4 weeks of the hypertension model, corresponding with the previously observed increase in arterial stiffness. These results clearly suggest an association between TG2 and the phenomenon of arterial rigidification.

INTRODUCTION

Transglutaminases (TGases) (EC 2.3.2.13) are a family of Ca^{2+}-dependent enzymes that catalyze an acyl transfer reaction from the γ-carboxamide group of a peptide-bound glutamine residue to the ε-amino group of a peptide-bound lysine residue, resulting in the formation of an isopeptidic amide bond that may crosslink peptides or proteins (Figure 1). Acyl transfer from glutamine to other primary amines and even water can also be mediated by TGases (Achyuthan et al., 1993; Folk and Cole, 1966; Greenberg et al., 1991). Mammalian TGases from tissue, epidermis, and plasma have been extensively characterized. Of these, tissue TGase (tissue transglutaminase [TG2]) has been shown to participate in biological processes such as endocytosis (Davies et al., 1980; Levitzki et al., 1980), apoptosis (Fesus et al., 1987), and cell growth regulation (Birckbichler et al., 1983). TG2 is mostly a cytosolic protein, but it has also been detected in the nucleus (Lesort et al., 1998) and can be secreted from the cell. Outside the cell, it plays one of its most important biological roles, crosslinking the extracellular matrix, thus making it less susceptible to proteolytic degradation (Aeschlimann and Thomazy, 2000). When TGase-mediated crosslinking activity is not carefully regulated, it may also be involved in a number of physiological disorders, such as acne (De Young et al., 1984), the formation of cataracts (Azari et al., 1981), immune system diseases (Fésüs, 1982), psoriasis (Schroeder et al., 1992), Alzheimer's disease (Norlund et al., 1999; Selkoe et al., 1982), Huntington's disease (Dedeoglu et al., 2002; Mastroberardino et al., 2002), Celiac disease (Piper et al., 2002), and cancer metastasis (Choi et al., 2005; Mehta, 2009).

TG2 has also been implicated in fibrosis (Griffin et al., 1979; Johnson et al., 2007; Small et al., 1999) and vascular calcification (Faverman et al., 2008; Johnson et al., 2008; Kaartinen et al., 2007). In large conduit arteries these two phenomena lead to a common feature of aging known as arterial stiffness. Vascular calcification is an active phenomenon involving the modulation of matrix Gla protein (Schurgers et al., 2008) and the phenotypic modulation of vascular smooth muscle cells (Shanahan et al., 2000). On the other hand, fibrosis may be explained by an increased collagen/elastin ratio in the extracellular matrix (Johnson et al., 2001). As we described previously this is due to elastin degradation (Bouvet et al., 2008) as well as the accumulation of collagen (Essalihi et al., 2007). TGase has been shown to participate in this phenomenon by crosslinking collagen in the extracellular matrix (Ientile et al., 2007; Johnson et al., 1997, 2007). The collagen network being rather rigid, its accumulation in arteries has been associated with increased vascular stiffness (Arribas et al., 2006; Bruel et al., 1998; Safar et al., 2003; Zieman et al., 2005).

The hemodynamic consequences of arterial stiffening are an increased systolic blood pressure, unchanged or slightly reduced diastolic blood pressure, increased pulse pressure, and the development of isolated systolic hypertension (ISH). We have developed a rat model of ISH, known as the warfarin/vitamin K (WVK) model, which mimics the physiopathological process of the disease observed in man (Bouvet et al., 2008; Essalihi et al., 2003, 2004, 2005). It consists in blocking the vitamin K-dependant maturation of a physiological inhibitor of calcification, matrix Gla protein, with warfarin, while preventing the rats from bleeding with the concomitant injection of Vitamin K1. With this model we obtain an elevation of vascular calcification, collagen content, and vascular stiffening within 4 weeks of treatments.

TG2 is involved in vascular calcification and collagen accumulation. These phenomena are known to cause arterial stiffening and occur in ISH. Therefore, our working hypothesis is that TG2 is involved in the stiffening of large arteries associated with ISH. Interrogation of the putative role of TG2 in arterial rigidification requires a sensitive method for detecting active TG2 in samples of arterial tissue. To that end we have designed substrate analog probes that are capable of reacting with TG2,

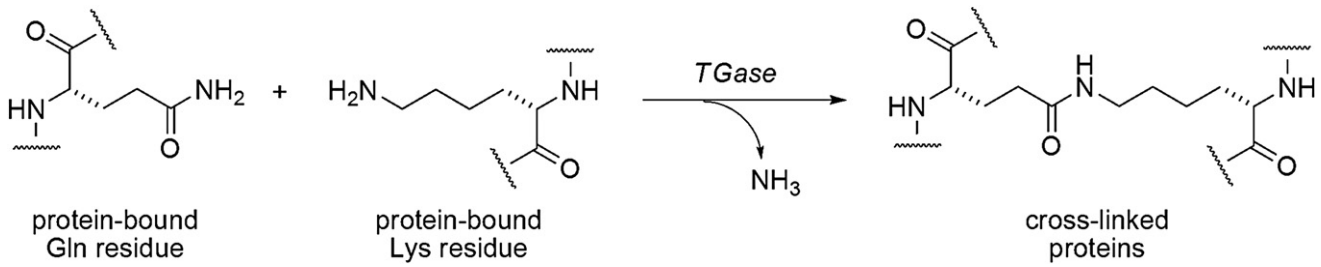

Figure 1. TGase-Mediated Protein Crosslinking

leading to its efficient fluorescent labeling. Furthermore, the use of one of these probes (**1**, Figure 2) in a rat ISH model allows an association to be made between TG2 activity and arterial rigidification.

RESULTS AND DISCUSSION

Probe Design and Synthesis

Many irreversible inhibitors of TG2 have been developed, based on a simple dipeptidic scaffold resembling the commonly used acyl-donor substrate, Cbz-Gln-Gly (Folk and Chung, 1985), bearing a reactive electrophilic group such as dihydroisoxazole (Choi et al., 2005), thiadiazole (Marrano et al., 2001), epoxide (Marrano et al., 2001), chloroacetamide (Pardin et al., 2006), maleimide (Halim et al., 2007), or α,β-unsaturated amide (de Macédo et al., 2002). These amides are among the most potent irreversible TGase inhibitors, having k_{inact}/K_I values exceeding 10^6 $M^{-1}min^{-1}$, attesting to the reactivity of an acrylamide group properly positioned in the TG2 active site. In a series of dipeptide acrylamide inhibitors, we have previously examined the effect of the length of the acrylamide-bearing side chain. This study convincingly demonstrated the superior reactivity and affinity of the dipeptide whose side chain comprises four methylene units, in $^{\varepsilon}N$-acryloyl lysine derivative **2** (Figure 2).

In order to be useful as a specific activity probe, an irreversible inhibitor must be selective for its target enzyme. In this light we designed a probe based on an extended peptide sequence that should show high affinity and selectivity for TG2. Our preliminary efforts to this end consisted of a simple sequence alignment of native proteins known to serve as high-affinity substrates for TG2. Namely, flanking amino acid sequences were compared between the glutamine-donor substrates pro-elafin peptide (Sohn et al., 2003) (KVLDGQDP) and gliadin peptide (Hausch et al., 2003) (PQPQLPY). We reasoned that the sequence PNPQLPF should confer excellent affinity for TG2, while presenting only one reactive Gln residue, potentially simplifying subsequent analyses. Interestingly, this sequence was found to conform roughly to the patterns predicted by Fésüs (Keresztessy et al., 2006) and Hitomi (Sugimura et al., 2006) upon analysis of TG2 reactivity with libraries of phage-displayed peptides. Our PNPQLPF sequence was then validated for in vivo reactivity by Lin and Ting (2006), who used it as a donor-substrate sequence in a TG2-mediated cell-surface labeling application. Finally, it is important to note the success that Khosla and coworkers (Hausch et al., 2003) have achieved with this approach. By inserting a 6-diazo-5-oxo-norleucine residue in the place of the second, reactive Gln residue in a high-affinity sequence based on a gliadin peptide, they designed the extended peptidic inhibitor Ac-PQP-DON-LPF-NH_2 (**3**, Figure 2) that reacts as efficiently as any small molecule inhibitor (k_{inact}/K_I = 2.9 × 10^6 $M^{-1}min^{-1}$). More recently, Khosla and coworkers (Pinkas et al., 2007) have shown that a truncated version of this inhibitor, namely Ac-P-DON-LPF-NH_2, reacts even more efficiently (k_{inact}/K_I = 8.3 × 10^6 $M^{-1}min^{-1}$).

Rhodamine B was chosen as a fluorophore for conjugation to the peptidic inhibitor sequence due to its high quantum yield and

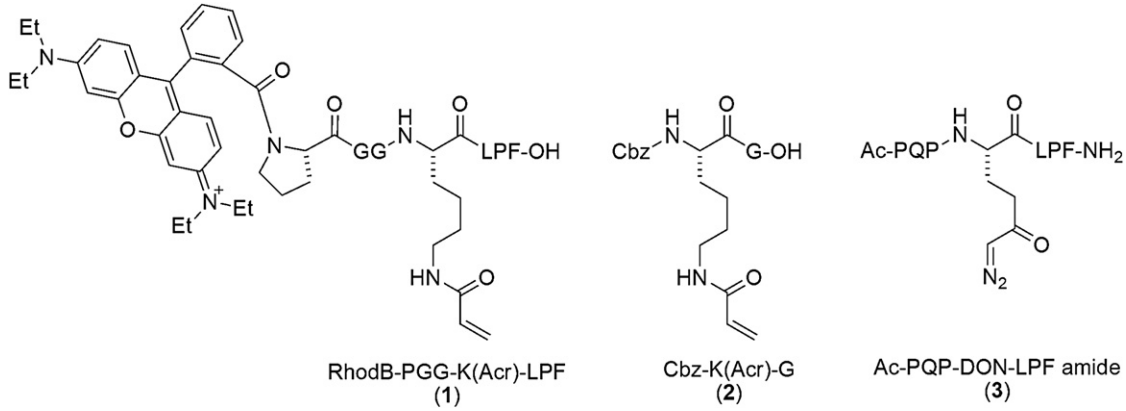

Figure 2. Rhodamine Probe 1 Used in This Work, Based on Previously Reported Irreversible Inhibitors 2 (de Macédo et al., 2002) and 3 (Pinkas et al., 2007)

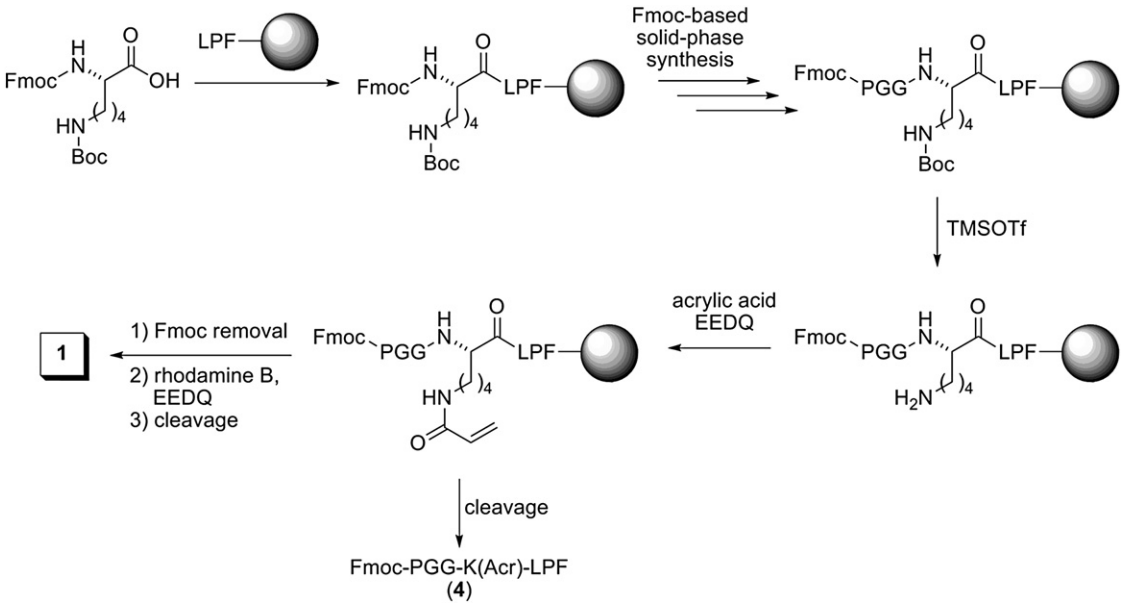

Figure 3. Solid-Phase Synthesis of Rhodamine Labeling Agent 1 and Control Compound 4

red emission, easily distinguishable from intrinsic cellular fluorescence. Furthermore, free rhodamine B is affordable, and its incorporation into a peptide sequence can be achieved through straightforward coupling procedures. In order to ensure that the fluorophore does not decrease the affinity of the peptide sequence for TG2 and that the adjacent peptide does not quench the fluorescence of the fluorophore, it was deemed necessary to attach the rhodamine to the peptide sequence through a spacer moiety. It has been reported that secondary amides of rhodamine are less fluorescent than their parent acid, presumably due to lactamisation. For this reason, the rhodamine moiety of inhibitor **1** was attached to the peptide sequence through a tertiary amide linkage with a proline residue. The nonfluorescent control compound **4** (Figure 3) was designed according to the same criteria, having the same reactive electrophile, substrate peptide sequence, and spacer sequence as inhibitor **1** but lacking the rhodamine B fluorophore.

To facilitate the preparation of these labeling agents, a strategy was developed to allow their synthesis on solid support (Figure 3). In general the devised synthetic route follows typical Fmoc-based peptide synthesis using Wang resin. Notably, the approach shown in Figure 3 allows the acryloyl group to be added to the ε-amino group of the Lys residue, without requiring cleavage from the resin. $^{\alpha}$*N*-Fmoc-$^{\varepsilon}$*N*-Boc-protected Lys was first prepared from a known protocol (Albericio et al., 1990) and then added to the resin-bound LPF tripeptide. Removal of the Boc group from the side chain of the doubly protected residue, without cleavage from the resin, was critical to this approach. This was achieved using TMSOTf, according to the procedure published by Lejeune et al. (2003). The acryloyl group was then added using acrylic acid and the coupling agent EEDQ, in the absence of base. These conditions were found to be superior to addition of acrylic anhydride, for example, giving an excellent yield without degradation of the electrophilic acryloyl group. Our procedure for Fmoc-based peptide coupling did not affect the integrity of the acryloyl group either, allowing a peptide spacer sequence to be added subsequently. Finally, the rhodamine fluorophore was added to the *N*-terminal of the peptide chain in excellent yield, using the same mild coupling conditions as for the addition of the acryloyl group. After cleavage from the resin, peptides were purified by preparative HPLC prior to kinetic evaluation or application.

The effect of the spacer sequence on the fluorescence of the rhodamine probe was also studied. Two additional probes were prepared, where the *N*-terminal proline residue of peptides **1** and **4** was replaced with glycine, resulting in peptides having spacer sequences GGG and numbered **5** and **6**, respectively (Table 1). The fluorescence of probe **1**, having a tertiary amide rhodamine linkage, was found to be comparable to free rhodamine B. However, peptide **5**, wherein the rhodamine moiety is attached to the peptide through a secondary amide, was found to be 13-fold less fluorescent. This is consistent with the putative formation of a lactam isomer having a significantly lower quantum yield (Adamczyk and Grote, 2000).

Finally, a negative control compound was prepared, bearing a rhodamine B moiety, but with a glycine residue in place of the electrophilic acryloyl-lysine residue. This control compound (RhodB-PGG-G-LPF-OH, **7**) was synthesized on solid support

Table 1. Kinetic Parameters Measured for TG2 Affinity Labels Studied Herein

Compound	R =	X =	k_{inact} (min^{-1})	K_I (μM)	k_{inact} / K_I (μM^{-1} min^{-1})
1	rhodamine B	Pro	0.68 ± 0.20	79 ± 44	0.009 ± 0.008
4	Fmoc	Pro	0.46 ± 0.08	42 ± 17	0.011 ± 0.006
5	rhodamine B	Gly	0.19 ± 0.02	6 ± 2	0.032 ± 0.014
6	Fmoc	Gly	0.36 ± 0.06	22 ± 8	0.016 ± 0.008

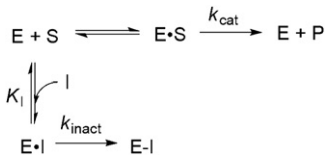

Figure 4. Kinetic Scheme for Irreversible Inhibition in the Presence of Substrate

according to methods similar to those shown in Figure 3 (see Experimental Procedures).

Kinetic Characterization

The affinity and reactivity of our probes were then determined in vitro. The reaction of recombinant guinea pig liver TG2, expressed and purified according to a published procedure (Gillet et al., 2004), with a chromogenic dipeptide substrate (de Macédo et al., 2000) showed a mono-exponential decrease in rate upon addition of peptidic inhibitors studied herein, consistent with the simplified kinetic scheme shown in Figure 4. First-order rate constants were measured for this loss of activity and fitted as a function of varied inhibitor concentration, taking into account the observed protection offered by the presence of substrate (see Figure 4 and Equation 1 in Experimental Procedures). The kinetic parameters thus measured for the peptidic inhibitors studied herein are shown in Table 1.

From Table 1 it would appear that peptides **5** and **6**, having lower K_I values than their respective counterparts **1** and **4**, may be bound more tightly by TG2. Perhaps the GGG spacer sequence, being more conformationally mobile than the PGG spacer, allows for better placement of the bulky Fmoc or rhodamine groups. However, this improved binding does not result in significantly improved reactivity because all of the probes studied have comparable overall efficiency ratios (k_{inact}/K_I). These efficiency ratios are lower than those of the most efficient peptidic irreversible inhibitors (Hausch et al., 2003; Pinkas et al., 2007), but they are as high (Pardin et al., 2006) or higher (Halim et al., 2007) than those of many other irreversible inhibitors, suggesting that peptide **1** may be used effectively as a useful fluorescent probe for TG2 activity.

Labeling Selectivity

Ultimately, for compound **1** to be most useful as a probe, it should ideally be selective for TG2. In particular it is important to distinguish between the activities of TGases TG2 and Factor XIIIa. As described above, the peptide sequence of **1** was designed to display affinity for TG2 and to be less reactive with Factor XIIIa, according to previously reported observed sequence specificities (Sugimura et al., 2006). The targeted selectivity was evaluated by incubating probe **1** with purified TG2 and with commercial Factor XIIIa, followed by visualization of fluorescent labeling by SDS-PAGE. As shown in Figure 5, probe **1** does not react significantly with Factor XIIIa (Figure 5A), but it reacts strongly with TG2 (Figure 5B), as intended. Furthermore, no reaction with TG2 was detected in the absence of added calcium (Figure 5C), confirming that the labeling reaction was indeed dependent on the native, calcium-dependent TG2 reaction.

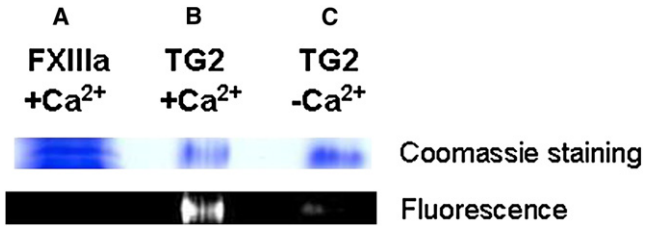

Figure 5. SDS-PAGE Analysis of Labeling Selectivity

Incubation of activated Factor XIIIa with compound **1** (30 min, 37°C) reveals no fluorescent labeling (lane A), whereas incubation with TG2 results in strong fluorescent labeling (lane B), but not in the absence of added calcium (lane C). See Experimental Procedures for details.

Tissue Staining and Biological Implication

In our model of ISH, arterial stiffness appears between the third and fourth week of WVK treatment (Essalihi et al., 2007). Indeed, calcification is usually increased first, followed closely by fibrosis, which leads to the stiffening of the artery. Therefore, we stained aortic tissue sections obtained from rats receiving this treatment for 1, 2, 3, and 4 weeks, while controls remained untreated. We first investigated control tissues, where no specific fluorescence could be detected, using compound **1** as a probe (Figure 6A). At one and two weeks of treatment (WVK1 and WVK2), some staining could be detected between the elastic lamellae of the aortic wall (Figures 6B and 6C). After 3 weeks of treatment (WVK3), we observed an interesting phenomenon. Indeed, aortic staining seemed to have moved from between elastic lamellae in the media of the artery to areas of undulated elastic lamellae present in the outer media, adjacent to the adventitia (Figure 6D). As we have shown previously, these regions correspond to areas of calcification, where elastic lamellae are fixed by hydroxyapatite crystals into an undulated form, as detected by von Kossa staining (Essalihi et al., 2005). This is also where fibrosis first appears when we stain these sections for collagen (Essalihi et al., 2007). Furthermore, at 4 weeks of treatment (WVK4), where calcification is at its maximum, but also when fibrosis is significantly elevated in the vascular wall (Essalihi et al., 2007), TG2 staining with compound **1** was now strictly associated with these undulated, calcified areas (Figure 6E). This suggests an association between calcification and TGase activity. Looking at the literature, we have no doubt that the role played by TG2 in these areas is pro-calcifying and pro-fibrotic by nature. However, further studies are necessary to confirm what is, at this point, only hypothetical in this model. To make sure that rhodamine was not staining the tissue nonspecifically, we used a control compound, **7**, that is coupled to rhodamine but does not react with TG2. When aortic sections were incubated with this compound, we did not detect any fluorescence (Figure 6F). Furthermore, to test for the specificity of compound **1**, we preincubated the sections with control compound **4**, which binds to TG2 but is not coupled to rhodamine. This allowed us to saturate the binding sites of compound **1** on active TG2. We then incubated the sections with compound **1** and did not detect significant fluorescence (Figure 6G) relative to sections treated only with compound **1**, indicative of the specificity of the staining method.

Therefore, we could detect an increased TG2 activity after as little as 1 week of treatment. Increasing the duration of treatment

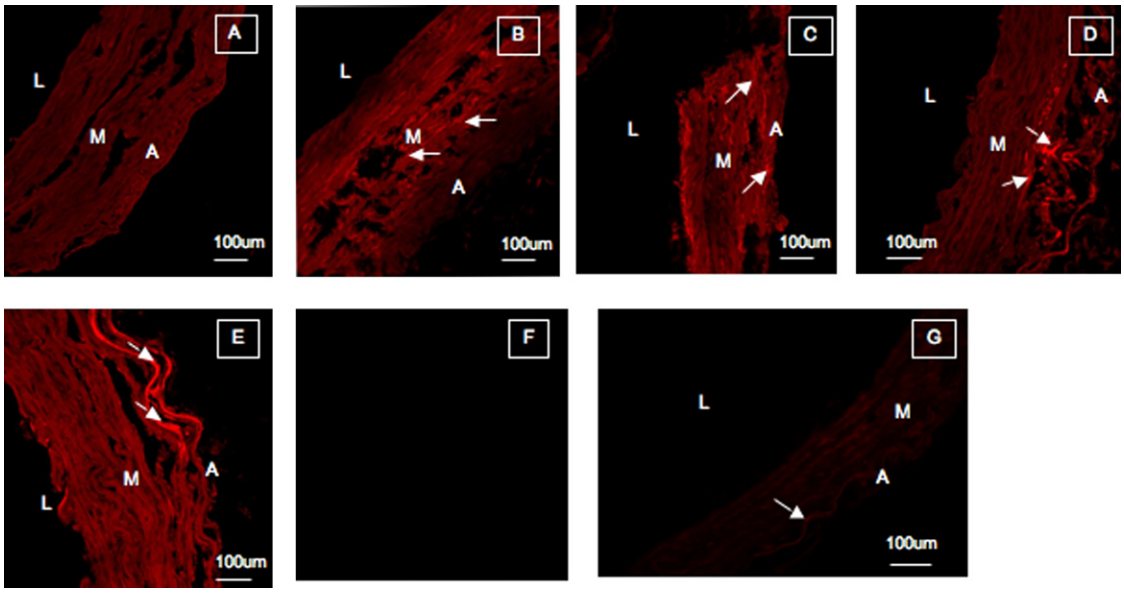

Figure 6. Fluorescent Staining of Aortic TG2

Staining of aortic tissues using irreversible TG2 inhibitors as fluorescent probes on control rats (A), WVK1 rats (B), WVK2 rats (C), WVK3 rats (D), and WVK4 rats (E). (F) Negative control using unreactive rhodamine derivative **7** on WVK4 rats. (G) Preincubation of compound **4** followed by incubation of compound **1** to determine the specificity of compound **1** staining on WVK4 rats. Arrows point to areas of intense TG2 labeling. A, adventitia; L, lumen; M, media of the aortic wall.

led to a staining pattern that was associated with areas of calcification and fibrosis. This suggests that TG2 activity is increased during the process of calcification and fibrosis associated with arterial stiffness and ISH. In future work it would be interesting to use these same irreversible inhibitors in the context of ISH, but as blocking agents rather than probes, to measure their impact on calcification, fibrosis, and arterial stiffness.

SIGNIFICANCE

New fluorescent irreversible inhibitors were designed as labeling agents for TG2. These inhibitors were based on a peptidic sequence designed to confer affinity for TG2 and selectivity over Factor XIIIa, as demonstrated by SDS-PAGE. As such, these inhibitors may be useful for "chemical knockout" experiments intended to distinguish the biological activities of the two closely related TGases. The fluorescence of the inhibitors presented herein was also optimized with respect to the spacer fragment that links the rhodamine B fluorophore to the peptide sequence. The most fluorescent inhibitor was then used to probe TG2 activity in a WVK rat model for ISH. Fluorescent staining of aortic tissue revealed that over a 4 week period, TG2 activity increases in parallel with arterial stiffness, suggesting an association between TG2 activity and arterial rigidification.

EXPERIMENTAL PROCEDURES

General Synthesis

All Fmoc-protected amino acids, resins, and coupling reagents were purchased from GL Biochem; Wang resin was purchased from NovaBiochem. All other reagents were obtained from Sigma-Aldrich. Reactions requiring anhydrous conditions were carried out under a dry nitrogen atmosphere employing conventional benchtop techniques. ^{1}H- and ^{13}C-NMR spectra were recorded on AMXR400 and AMX300 spectrometers and were referenced to the residual proton or ^{13}C signal of the solvent. Mass spectra were determined by FAB+ ionization on an AutoSpec Q spectrometer at the Regional Mass Spectrometry Centre at the Université de Montréal.

Reactor tubes for solid-phase peptide synthesis were obtained from Supelco, and shaking was performed on a shaker. All resins were swelled in DMF, and washing steps were performed using CH_2Cl_2 and DMF (EMD Chemicals). Purification of all peptides was performed using a preparative HPLC method. Mass spectral data (MS, LCMS) were obtained using two different columns—column A: Gemini C18, 150 × 4.6 mm, 5 m (Phenomenex, Torrance, CA); and column B: Synergi Polar-RP, 150 × 4.6 mm, 4 m (Phenomenex, Torrance, CA). Crude peptides were purified using a preparative Synergi Polar-RP, 100 × 21.20 mm column (Phenomenex, Torrance, CA) on a Varian (Prep Star) HPLC system at the Regional Mass Spectrometry Centre at the Université de Montréal.

General Procedure for Fmoc Peptide Synthesis of Irreversible Inhibitors

All peptides were synthesized using standard solid-phase Fmoc chemistry. Briefly, the first Fmoc protected amino acid (5.5 mmol) was coupled to Wang resin (1.1 mmol) using DIC (5.5 mmol) and DMAP (0.11 mmol) in DMF (5 resin volumes). The level of loading of the amino acid on the resin after the first coupling step was determined by spectroscopic measurement of the UV absorbance of the piperidine dibenzofulvalene adduct formed during Fmoc deprotection. This loading level was used as the resin loading capacity for all subsequent steps. The remaining free hydroxyl functionalities were capped by treating the resin with a mixture of acetic anhydride/pyridine (2:3), followed by shaking for 2 hr. After washing with DMF (three times with 10 resin volumes), DCM (three times with 10 resin volumes), and ether (three times with 10 resin volumes), the Fmoc group was removed by incubating three times with piperidine in DMF (20% v/v; 10 resin volumes) for 5 min, followed by washing with DMF (three times with 10 resin volumes), DCM (three times with 10 resin volumes), and ether (three times with 10 resin volumes) in preparation for the next amide coupling. Deprotection was verified by a positive Kaiser test on a sample of a few beads. Then each Fmoc protected amino acid (1.7 mmol) was coupled to Wang resin preloaded with the necessary carboxyl-terminal amino acid (0.68 mmol) in DMF (5 resin volumes) using

HOBT (1.7 mmol) and DIC (1.7 mmol). This operation was performed twice for 30 min. Coupling was verified by a negative Kaiser test on a sample of a few beads. The peptide was then cleaved from the resin (1 g) by incubating with TFA:DCM (1:1) for 2 hr. The peptide was precipitated from the cleavage solution using diethyl ether and hexane, and its purity was determined by HPLC using two different columns—column A: Gemini C18, 150 × 4.6 mm, 5μ (Phenomenex, Torrance, CA); and column B: Synergi Polar-RP, 150 × 4.6 mm, 4μ (Phenomenex, Torrance, CA). The crude peptide was purified using a preparative Synergi Polar-RP, 100 × 21.20 mm column (Phenomenex, Torrance, CA) on a Varian (Prep Star) HPLC system.

Boc Deprotection Protocol

To a reactor containing 1 g of the Wang resin-supported Fmoc-peptide (0.68 mmol, according to the measured loading level) were added 30 ml of deprotection mixture, freshly prepared from 470 μl TEA (2 eq.), 1.09 ml of TMSOTf (0.2 M), and 28.44 ml of anhydrous DCE. The resin was shaken for 10 min, then filtered and washed with 5 × 5 ml of DCM, 2 × 5 ml of DIEA 10% in DCM, and 3 × 5 ml of DCE. Deprotection was carried out for another 10 min with a fresh deprotection mixture. The resin was filtered then washed with 5 × 5 ml of DCM, 2 × 5 ml of DIEA 10% in DCM, 2 × 5 ml of DCM, 2 × 5 ml of DMF, and 2 × 5 ml of Et_2O. Deprotection was verified by a positive Kaiser test on a sample of a few beads.

Acrylation and Rhodamine B-Coupling Protocol

To the Wang resin-supported peptide (1 g, 0.68 mmol), either Fmoc protected in the case of acrylation or deprotected in the case of rhodamine B coupling, swollen in anhydrous DCM (5 resin volumes), was added acrylic acid (1.7 mmol) and EEDQ (1.7 mmol). The reaction mixture was shaken for 1 hr, followed by washing with DMF (three times with 10 resin volumes), DCM (three times with 10 resin volumes), and ether (three times with 10 resin volumes). This operation was performed twice.

HPLC Analysis and Purification

For HPLC analysis, the peptide was cleaved from the resin as described in General Procedure for Fmoc Peptide Synthesis of Irreversible Inhibitors. The crude material was purified by preparative Synergi Polar-RP (100 × 21.20 mm) column, on a Varian (Prep Star) HPLC system using 80%–95% of MeOH in water as eluant, a flow rate of 8 ml/min, and the detector set at 254 nm. The collected fractions were freeze-dried to give the peptide in the form of a powder. The areas under the peaks were determined using LC/MSD Chem Station (Agilent Technologies).

Synthesis of Irreversible Inhibitors

RhodamineB-prolinyl-glycinyl-glycinyl-lysinyl(acryloyl)-leucinyl-prolinyl-phenylalaninate (1).This peptide was cleaved from the resin and purified by preparative HPLC as described previously. The collected fractions were freeze-dried to give the desired irreversible peptidic inhibitor **1** as a pink powder (overall yield: 10%; 98% purity by column A, 96% purity by column B). HRMS m/z ($M+H^+$): calcd 1193.63938; found 1193.63908.

Fmoc-Prolinyl-glycinyl-glycinyl-lysinyl(acryloyl)-leucinyl-prolinyl-phenylalaninate (4).This peptide was cleaved from the resin and purified by preparative HPLC as described previously. The collected fractions were freeze-dried to give the desired irreversible peptidic inhibitor **4** as a white powder (8% overall yield; 91% purity by column A, 90% purity by column B). HRMS m/z ($M+H^+$): calcd 991.49238; found 991.49072.

Fmoc-Glycinyl-glycinyl-glycinyl-lysinyl(acryloyl)-leucinyl-prolinyl-phenylalaninate (5).This peptide was cleaved from the resin and purified by preparative HPLC as described previously. The collected fractions were freeze-dried to give the desired irreversible peptidic inhibitor **5** (6% of yield ; 98% purity by column A, 99.9% purity by column B) as a white powder. HRMS m/z ($M+H^+$): calcd 951.46108; found 951.46215.

RhodamineB-glycinyl-glycinyl-glycinyl-lysinyl(acryloyl)-leucinyl-prolinyl-phenylalaninate (6).This peptide was cleaved from the resin and purified by preparative HPLC as described previously. The collected fractions were freeze-dried to give the desired irreversible peptidic inhibitor **6** (yield: 10%; 81% purity by column A, 80% purity by column B) as a pink powder. HRMS m/z ($M+H^+$): calcd 1153.60808; found 1153.60589.RhodamineB-prolinyl-glycinyl-glycinyl-glycinyl-leucinyl-prolinyl-phenylalaninylate (7).This peptide was cleaved from the resin and purified by preparative HPLC as described previously. The collected fractions were freeze-dried to give the desired control probe **7** as a pink powder (yield: 30%; 99% purity by column A, 98% purity by column B). HRMS m/z ($M+H^+$): calcd 1068.55532; found 1068.55472.

Kinetic Methods for Irreversible Inhibition

All assays were performed in triplicate. Kinetic runs were recorded on a UV-visible spectrophotometer at 405 nm and 25°C, in a buffer composed of 50 mM $CaCl_2$, 50 μM EDTA, and 0.1 M MOPS (pH 7.0). All aqueous solutions were prepared using deionized water. All kinetic assays were carried out using 900 μl of buffer, 50 μl of 0.15 mg/ml TGase, 25 μl of the chromogenic substrate Cbz-Glu(γ-*p*-nitrophenyl ester)Gly (Leblanc et al., 2001) dissolved in DMF (54 μM, corresponding to 6-fold K_M), and 25 μl of inhibitor. Final concentrations of inhibitors ranged from 10 μM to the solubility limit of each compound. Stock solutions of the inhibitors were also prepared in DMF such that the final concentration of this co-solvent was constant at 5% v/v. Kinetic runs were initiated by enzyme addition, and evaluation was carried out by the method of Stone and Hofsteenge (1985), as described previously (de Macédo et al., 2002; Marrano et al., 2001). Mono-exponential time-dependent inactivation was observed for all of the inhibitors studied herein. Observed first-order rate constants of inactivation were determined from nonlinear regression, using a mono-exponential model. These rate constants were in turn fit to Equation 1 by nonlinear regression, providing the kinetic parameters k_{inact} and K_I as defined in Figure 4 and shown in Table 1.

$$k_{obs} = \frac{k_{inact}[I]}{[I] + K_I\left(1 + \frac{[S]}{K_M}\right)}. \quad (1)$$

Enzyme Preparation

Recombinant guinea pig liver TG2 was overexpressed and purified from *E. coli* following our previously published procedure (Gillet et al., 2004). The purified TG2 solution used in all assays had a specific activity of 30 U/mg in 25 mM Tris-acetate (pH 7) according to the hydroxamate activity assay (Nemes et al., 2005), in which Cbz-L-Gln-Gly and hydroxylamine are used as acyl-donor and acyl-acceptor substrates, respectively. Recombinant human TG2, used in the selectivity tests, was expressed and purified as reported previously (Piper et al., 2002). Its activity was verified using a previously reported chromogenic activity assay (Leblanc et al., 2001). Factor XIII was purchased from Zedira (Darmstadt, Germany). It was activated using thrombin and its activity verified by a fluorogenic assay, according to the supplier's protocols.

Selectivity Tests

Parallel incubation experiments were performed in three 1.5 ml Eppendorf tubes. To the first was added Factor XIII (3 mg/ml (activated with 0.3 NIH units of thrombin), in 56.8 mM Tris (pH 7.5), 11.36 mM $CaCl_2$, 113.6 mM NaCl, 0.113% w/v PEG 8000, 5.68 mM GlyOMe●HCl, 5.68 mg/l hexadimethrine bromide, and compound **1** (90 μM dissolved in DMF, 0.9% final vol/vol). To the second was added human TG2 (0.868 mg/ml in 25 mM Tris [pH 7.2], 150 mM NaCl, 1 mM EDTA, and 1 mM TCEP) in the presence of calcium (0.6 M) and compound **1** (90 μM dissolved in DMF, 0.9% final vol/vol). The third tube was identical to the second, but with 5 mM EDTA and no added calcium. All three tubes were incubated for 30 min at 37°C, then analyzed by 10% SDS-PAGE. The resulting gel was exposed under a trans-UV lamp to determine fluorescent labeling and then stained with Coomassie blue to reveal protein.

Animal Treatments

Male Wistar rats weighing 175–200 g (n = 9 per group) were obtained from Charles River Breeding Laboratories (Saint-Constant, QC, Canada). They received warfarin (20 mg/kg/day in drinking water) and vitamin K (phylloquinone, 15 mg/kg/day sc injection) (WVK) during 1, 2, 3, and 4 weeks. Dosages were adjusted every second day. Control rats consisted of age-matched untreated rats. All animal experiments were approved by the Animal Care and Use Committee of Université de Montréal.

Tissue Preparation

Animals were sacrificed with a lethal dose of pentobarbital (65 mg/kg), and the aorta was harvested. A small section (0.5–1 cm) of aorta was frozen at −80°C in Tissue-Tek OCT compound (Sakura Finetek Inc., Torrance, CA). These aorta sections were later cut into 10 μm thick cryosections with a cryostat (Leica Microsystems, model CM3050S, Richmond Hill, ON, Canada), collected on Colorfrost/Plus Microscope slides (Fisher scientific, Ottawa, ON, Canada), and kept at −20°C.

Tissue Staining

Tissue slides were allowed to thaw at room temperature for 20 min. OCT was removed, and tissues were permeabilized in PBS containing 0.1% triton for 20 min. Tissue sections were then circled using an ImmEdge PEN (Vector Laboratories, Burlingame, CA). A 1 mM solution of compound **1** was prepared in a buffer containing 0.1 M Tris HCl (pH 7.5), 0.15 M NaCl, and 5 mM $CaCl_2$ and applied to the tissue sections for 15 min at 37°C. Slides were then rinsed four times (5 min each) under agitation in PBS. After rinsing in distilled water for 5 min, slides were dried briefly before applying a solution of Mowiol/*p*-phenylenediamine (9:1 vol/vol) (Calbiochem, San Diego, CA, USA, and Sigma-Aldrich, Canada, respectively) to prevent bleaching. As a negative control, we applied 1 mM of an inactive form of the inhibitor, compound **7**, that is also coupled to rhodamine. Furthermore, to make sure that compound **1** does not bind nonspecifically in the tissue, we applied 5 mM of control compound **4**, an irreversible inhibitor that is not coupled to rhodamine, for 45 min at 37°C, before applying 1 mM of the normal rhodamine-coupled inhibitor (**1**), to the same section. Because compound **1** binds to the active form of TG2, fluorescence was evaluated as an index of TG2 activity. To do so, slides were photographed with a fluorescent microscope (Axioskop 40, Carl Zeiss Canada Ltd., Toronto, Ontario, Canada, with SPOT RT Slider, Diagnostic Instruments Inc., Sterling Heights, MI, USA).

ACKNOWLEDGMENTS

This study was supported by the Canadian Institutes for Health Research (CIHR), the Natural Sciences and Engineering Research Council of Canada (NSERC), and the Groupe de recherche universitaire sur les médicaments (GRUM). S.M. received a studentship from the Fonds de Recherche en Santé du Québec (FRSQ). N.C. and A.M. are grateful for bursaries from GRUM.

Received: February 3, 2010
Revised: June 28, 2010
Accepted: June 30, 2010
Published: October 28, 2010

REFERENCES

Achyuthan, K.E., Slaughter, T.F., Santiago, M.A., Enghild, J.J., and Greenberg, C.S. (1993). Factor XIIIa-derived peptides inhibit transglutaminase activity. Localization of substrate recognition sites. J. Biol. Chem. *268*, 21284–21292.

Adamczyk, M., and Grote, J. (2000). Efficient synthesis of rhodamine conjugates through the 2′-position. Bioorg. Med. Chem. Lett. *10*, 1539–1541.

Aeschlimann, D., and Thomazy, V. (2000). Protein crosslinking in assembly and remodeling of extracellular matrices: the role of transglutaminase. Connect. Tissue Res. *41*, 1–27.

Albericio, F., Nicolas, E., Rizo, J., Ruiz-Gayo, M., Pedroso, E., and Giralt, E. (1990). Convenient syntheses of fluorenylmethyl-based side chain derivatives of glutamic and aspartic acids, lysine, and cysteine. Synthesis 1990 *2*, 119–122.

Arribas, S.M., Hinek, A., and Gonzalez, M.C. (2006). Elastic fibres and vascular structure in hypertension. Pharmacol. Ther. *111*, 771–791.

Azari, P., Rahim, I., and Clarkson, D.P. (1981). Transglutaminase activity in normal and hereditary cataractous rat lens and its partial purification. Curr. Eye Res. *1*, 463–469.

Birckbichler, P.J., Orr, G.R., Patterson, M.K., Conway, E., Carter, H.A., and Maxwell, M.D. (1983). Enhanced transglutaminase activity in transformed human lung fibroblast cells after exposure to sodium butyrate. Biochim. Biophys. Acta *763*, 27–34.

Bouvet, C., Moreau, S., Blanchette, J., de Blois, D., and Moreau, P. (2008). Sequential activation of matrix metalloproteinase 9 and transforming growth factor beta in arterial elastocalcinosis. Arterioscler. Thromb. Vasc. Biol. *28*, 856–862.

Bruel, A., Ortoft, G., and Oxlund, H. (1998). Inhibition of cross-links in collagen is associated with reduced stiffness of the aorta in young rats. Atherosclerosis *140*, 135–145.

Choi, K., Siegel, M., Piper, J.L., Yuan, L., Cho, E., Strnad, P., Omary, B., Rich, K.M., and Khosla, C. (2005). Chemistry and biology of dihydroisoxazole derivatives: selective inhibitors of human transglutaminase 2. Chem. Biol. *12*, 469–475.

Davies, P.J.A., Davies, D.R., Levitzki, A., Maxfield, F.R., Milhaud, P., Willingham, M.C., and Pastan, I.H. (1980). Transglutaminase is essential in receptor-mediated endocytosis of alpha 2-macroglobulin and polypeptide hormones. Nature *283*, 162–167.

de Macédo, P., Marrano, C., and Keillor, J.W. (2000). A direct and continuous spectrophotometric assay for transglutaminase mediated transpeptidation activity. Anal. Biochem. *285*, 16–20.

de Macédo, P., Marrano, C., and Keillor, J.W. (2002). Synthesis of dipeptide-bound epoxides and a,b-unsaturated amides as potential irreversible transglutaminase inhibitors. Bioorg. Med. Chem. *10*, 355–360.

De Young, L., Ballaron, S., and Epstein, W. (1984). Transglutaminase activity in human and rabbit ear comedogenesis: a histochemical study. J. Invest. Dermatol. *82*, 275–279.

Dedeoglu, A., Kubilus, J.K., Jeitner, T.M., Matson, S.A., Bogdanov, M., Kowall, N.W., Matson, W.R., Cooper, A.J., Ratan, R.R., Beal, M.F., et al. (2002). Therapeutic effects of cystamine in a murine model of Huntington's disease. J. Neurosci. *22*, 8942–8950.

Essalihi, R., Dao, H.H., Gilbert, L.A., Bouvet, C., Semerjian, Y., McKee, M.D., and Moreau, P. (2005). Regression of medial elastocalcinosis in rat aorta: a new vascular function for carbonic anhydrase. Circulation *112*, 1628–1635.

Essalihi, R., Dao, H.H., Yamaguchi, N., and Moreau, P. (2003). A new model of isolated systolic hypertension induced by chronic warfarin and vitamin K1 treatment. Am. J. Hypertens. *16*, 103–110.

Essalihi, R., Ouellette, V., Dao, H.H., McKee, M.D., and Moreau, P. (2004). Phenotypic modulation of vascular smooth muscle cells during medial arterial calcification: a role for endothelin? J. Cardiovasc. Pharmacol. *44* (*Suppl 1*), S147–S150.

Essalihi, R., Zandvliet, M.L., Moreau, S., Gilbert, L.A., Bouvet, C., Lenoel, C., Nekka, F., McKee, M.D., and Moreau, P. (2007). Distinct effects of amlodipine treatment on vascular elastocalcinosis and stiffness in a rat model of isolated systolic hypertension. J. Hypertens. *25*, 1879–1886.

Faverman, L., Mikhaylova, L., Malmquist, J., and Nurminskaya, M. (2008). Extracellular transglutaminase 2 activates beta-catenin signaling in calcifying vascular smooth muscle cells. FEBS Lett. *582*, 1552–1557.

Fésüs, L. (1982). Transglutaminase activation: significance with respect to immunologic phenomena. Surv. Immunol. Res. *1*, 297–304.

Fesus, L., Thomazy, V., and Falus, A. (1987). Induction and activation of tissue transglutaminase during programmed cell death. FEBS Lett. *224*, 104–108.

Folk, J.E., and Chung, S.I. (1985). Transglutaminases. Methods Enzymol. *113*, 358–375.

Folk, J.E., and Cole, P.W. (1966). Mechanism of action of guinea pig liver transglutaminase. I. Purification and properties of the enzyme: identification of a functional cysteine essential for activity. J. Biol. Chem. *241*, 5518–5525.

Gillet, S.M.F.G., Chica, R.A., Keillor, J.W., and Pelletier, J.N. (2004). Expression and rapid purification of highly active hexahistidine-tagged guinea pig liver transglutaminase. Protein Expr. Purif. *33*, 256–264.

Greenberg, C.S., Birchbichler, P.J., and Rice, R.H. (1991). Transglutaminases: multifunctional cross-linking enzymes that stabilize tissues. FASEB J. *5*, 3071–3077.

Griffin, M., Smith, L.L., and Wynne, J. (1979). Changes in transglutaminase activity in an experimental model of pulmonary fibrosis induced by paraquat. Br. J. Exp. Pathol. *60*, 653–661.

Halim, D., Caron, K., and Keillor, J.W. (2007). Synthesis and evaluation of peptidic maleimides as transglutaminase inhibitors. Bioorg. Med. Chem. Lett. *17*, 305–308.

Hausch, F., Halttunen, T., Maki, M., and Khosla, C. (2003). Design, synthesis, and evaluation of gluten peptide analogs as selective inhibitors of human tissue transglutaminase. Chem. Biol. *10*, 225–231.

Ientile, R., Caccamo, D., and Griffin, M. (2007). Tissue transglutaminase and the stress response. Amino Acids *33*, 385–394.

Johnson, T.S., Griffin, M., Thomas, G.L., Skill, J., Cox, A., Yang, B., Nicholas, B., Birckbichler, P.J., Muchaneta-Kubara, C., and Meguid El Nahas, A. (1997). The role of transglutaminase in the rat subtotal nephrectomy model of renal fibrosis. J. Clin. Invest. *99*, 2950–2960.

Johnson, C.P., Baugh, R., Wilson, C.A., and Burns, J. (2001). Age related changes in the tunica media of the vertebral artery: implications for the assessment of vessels injured by trauma. J. Clin. Pathol. *54*, 139–145.

Johnson, T.S., Fisher, M., Haylor, J.L., Hau, Z., Skill, N.J., Jones, R., Saint, R., Coutts, I., Vickers, M.E., El Nahas, A.M., and Griffin, M. (2007). Transglutaminase inhibition reduces fibrosis and preserves function in experimental chronic kidney disease. J. Am. Soc. Nephrol. *18*, 3078–3088.

Johnson, K.A., Polewski, M., and Terkeltaub, R.A. (2008). Transglutaminase 2 is central to induction of the arterial calcification program by smooth muscle cells. Circ. Res. *102*, 529–537.

Kaartinen, M.T., Murshed, M., Karsenty, G., and McKee, M.D. (2007). Osteopontin upregulation and polymerization by transglutaminase 2 in calcified arteries of Matrix Gla protein-deficient mice. J. Histochem. Cytochem. *55*, 375–386.

Keresztessy, Z., Csósz, E., Hársfalvi, J., Csomós, K., Gray, J., Lightowlers, R.N., Lakey, J.H., Balajthy, Z., and Fésüs, L. (2006). Phage display selection of efficient glutamine-donor substrate peptides for transglutaminase 2. Protein Sci. *15*, 2466–2480.

Leblanc, A., Gravel, C., Labelle, J., and Keillor, J.W. (2001). Kinetic studies of guinea pig liver transglutaminase reveal a general-base-catalyzed deacylation mechanism. Biochemistry *40*, 8335–8342.

Lejeune, V., Martinez, J., and Cavelier, F. (2003). Towards a selective Boc deprotection on acid cleavable Wang resin. Tetrahedron Lett. *44*, 4757–4759.

Lesort, M., Attanavanich, K., Zhang, J., and Johnson, G.V. (1998). Distinct nuclear localization and activity of tissue transglutaminase. J. Biol. Chem. *273*, 11991–11994.

Levitzki, A., Willingham, M., and Pastan, I.H. (1980). Evidence for participation of transglutaminase in receptor-mediated endocytosis. Proc. Natl. Acad. Sci. USA *77*, 2706–2710.

Marrano, C., de Macédo, P., and Keillor, J. (2001). Evaluation of novel dipeptide-bound a,b-unsaturated amides and epoxides as irreversible inhibitors of guinea pig liver transglutaminase. Bioorg. Med. Chem. *9*, 1923–1928.

Mastroberardino, P.G., Iannicola, C., Nardacci, R., Bernassola, F., De Laurenzi, V., Melino, G., Moreno, S., Pavone, F., Oliverio, S., Fesus, L., and Piacentini, M. (2002). "Tissue" transglutaminase ablation reduces neuronal death and prolongs survival in a mouse model of Huntington's disease. Cell Death Differ. *9*, 873–880.

Mehta, K. (2009). Biological and therapeutic significance of tissue transglutaminase in pancreatic cancer. Amino Acids *36*, 709–716.

Nemes, Z., Petrovski, G., and Fésüs, L. (2005). Tools for the detection and quantitation of protein transglutamination. Anal. Biochem. *342*, 1–10.

Norlund, M.A., Lee, J.M., Zainelli, G.M., and Muma, N.A. (1999). Elevated transglutaminase-induced bonds in PHF tau in Alzheimer's disease. Brain Res. *851*, 154–163.

Pardin, C., Gillet, S.M.F.G., and Keillor, J.W. (2006). Synthesis and evaluation of peptidic irreversible inhibitors of tissue transglutaminase. Bioorg. Med. Chem. *14*, 8379–8385.

Pinkas, D.M., Strop, P., Brunger, A.T., and Khosla, C. (2007). Transglutaminase 2 undergoes a large conformational change upon activation. PLoS Biol. *5* (12), e327.

Piper, J.L., Gray, G.M., and Khosla, C. (2002). High selectivity of human tissue transglutaminase for immunoactive gliadin peptides: implications for celiac sprue. Biochemistry *41*, 386–393.

Safar, M.E., Levy, B.I., and Struijker-Boudier, H. (2003). Current perspectives on arterial stiffness and pulse pressure in hypertension and cardiovascular diseases. Circulation *107*, 2864–2869.

Schroeder, W.T., Thacher, S.M., Stewart-Galetka, S., Annarella, M., Chema, D., Siciliano, M.J., Davies, P.J.A., Tang, H.Y., Sowa, B.A., and Duvic, M. (1992). Type I keratinocyte transglutaminase: expression in human skin and psoriasis. J. Invest. Dermatol. *99*, 27–34.

Schurgers, L.J., Cranenburg, E.C., and Vermeer, C. (2008). Matrix Gla-protein: the calcification inhibitor in need of vitamin K. Thromb. Haemost. *100*, 593–603.

Selkoe, D.J., Abraham, C., and Ihara, Y. (1982). Brain transglutaminase: in vitro crosslinking of human neurofilament proteins into insoluble polymers. Proc. Natl. Acad. Sci. USA *79*, 6070–6074.

Shanahan, C.M., Proudfoot, D., Tyson, K.L., Cary, N.R., Edmonds, M., and Weissberg, P.L. (2000). Expression of mineralisation-regulating proteins in association with human vascular calcification. Z. Kardiol. *89* (*Suppl 2*), 63–68.

Small, K., Feng, J.F., Lorenz, J., Donnelly, E.T., Yu, A., Im, M.J., Dorn, G.W., 2nd, and Liggett, S.B. (1999). Cardiac specific overexpression of transglutaminase II (G(h)) results in a unique hypertrophy phenotype independent of phospholipase C activation. J. Biol. Chem. *274*, 21291–21296.

Sohn, J., Kim, T., Young-Hee, Y., Kim, J., and Kim, S. (2003). Novel transglutaminase inhibitors reverse the inflammation of allergic conjunctivitis. J. Clin. Invest. *111*, 121–128.

Stone, S.R., and Hofsteenge, J. (1985). Specificity of activated human protein C. Biochem. J. *230*, 497–500.

Sugimura, Y., Hosono, M., Wada, F., Yoshimura, T., Maki, M., and Hitomi, K. (2006). Screening for the preferred substrate sequence of transglutaminase using a phage-displayed peptide library: identification of peptide substrates for TGASE 2 and Factor XIIIA. J. Biol. Chem. *281*, 17699–17706.

Lin, C.W., and Ting, A.Y. (2006). Transglutaminase-catalyzed site-specific conjugation of small-molecule probes to proteins in vitro and on the surface of living cells. J. Am. Chem. Soc. *128*, 4542–4543.

Zieman, S.J., Melenovsky, V., and Kass, D.A. (2005). Mechanisms, pathophysiology, and therapy of arterial stiffness. Arterioscler. Thromb. Vasc. Biol. *25*, 932–943.

